

Improving the Performance of Mobile Broadcasting Systems Using Multiple Base Stations and Distributed Space-Time Codes

Jan Mietzner* and Peter Adam Hoeher

Information and Coding Theory Lab (ICT), Faculty of Engineering, University of Kiel,
Kaiserstrasse 2, D-24143 Kiel, Germany.

Phone: +49 431 880-6133, Fax: +49 431 880-6128,

E-mail: {jm,ph}@tf.uni-kiel.de, URL: www-ict.tf.uni-kiel.de.

Abstract

The error performance of distributed space-time codes used for mobile broadcasting systems consisting of multiple base stations is analysed. The base stations are assumed to operate in a simulcast mode, i.e., they simultaneously transmit the same message using the same carrier frequency. Mobile users within the intersection of the coverage areas thus enjoy a small probability of shadowing and a high probability of at least one line-of-sight link. In effect, the base stations establish a virtual multiple-antenna system. The use of a distributed space-time code offers an additional spatial diversity gain. Considering a single user with a fixed (random) position, the impact of shadowing and line-of-sight components on the error performance of the system is analysed and compared with a conventional multiple-antenna system with co-located transmit antennas. Specifically, our analysis shows that already a single line-of-sight link significantly improves the overall system performance. In the case of shadowing, huge diversity gains are obtained in the distributed system. In a system with co-located transmitters, however, the performance improvements compared to a single-antenna system are rather small, when shadowing is taken into account. Altogether, it can be concluded that systems with distributed transmitters are typically superior to conventional multiple-antenna systems (due to macroscopic diversity), and that distributed space-time codes are superior to conventional simulcasting (due to microscopic diversity).

Keywords: Wireless communications, broadcasting, simulcasting, cooperative networks, shadowing, line-of-sight, diversity, distributed space-time codes, performance analysis.

*Corresponding author

1 Introduction

MOBILE radio systems are known to suffer from fading effects. However, system performance can be improved significantly by exploiting some sort of diversity. By means of multiple antennas, microscopic (small-scale) spatial diversity can be exploited, provided that the individual links from the transmit antenna(s) to the receive antenna(s) fade independently. This yields significant gains compared to systems with just a single antenna at either end of the wireless link. Multiple antennas at the transmitter side allow for a two-dimensional coding in time and space (i.e., across the individual antennas), which is commonly known as space-time coding, e.g. [1]-[4]. In addition, multiple receive antennas can be used so as to further improve system performance. If multiple antennas are only available at the receiver side, spatial diversity can be utilised by means of appropriate linear combining techniques [5].

Spatial diversity can also be exploited in cooperative wireless networks, e.g. [6]-[12]. In such networks, multiple (single-antenna) nodes share their antennas, for example by using a distributed space-time coding scheme. By this means, a virtual multiple-antenna system is established. The concept of cooperative wireless networks has recently gained considerable attention, because cooperating nodes build the basis of any ad-hoc network and promise benefits also for other types of networks, such as cellular networks [11]. Examples for cooperative wireless networks include simulcast networks [6] and relay-assisted networks [7]-[12].

***** Fig. 1 about here *****

In this paper, simulcast networks are considered that consist of multiple base stations, see Fig. 1. Simulcast networks are normally employed for broadcasting or for paging applications. Conventionally, simulcasting means that the base stations simultaneously transmit the same signal on the same carrier frequency. Mobile users within the intersection of the coverage areas are thus provided with a comparably small probability of shadowing¹ and a high probability of at least one line-of-sight link (macroscopic spatial diversity). However, conventional simulcasting does not yield any microscopic spatial diversity gain [6]. In this paper, we assume that the base stations use a distributed

¹Shadowing is caused by large-scale objects situated between the base station(s) and the mobile receiver.

space-time coding scheme in order to provide an additional microscopic diversity gain.

The outline of the paper is as follows: The system model under consideration is introduced in Section 2. In Section 3, the error performance of a distributed space-time coding scheme is determined analytically for a single receiver with fixed random position. The resulting error performance is compared to a conventional multiple-antenna system with co-located transmitters, and the influence of shadowing and line-of-sight components is studied. It is shown that systems with distributed transmitters are typically superior to conventional multiple-antenna systems, and that distributed space-time codes are superior to conventional simulcasting. To the best of the authors' knowledge, such a comparative study for distributed space-time codes with regard to shadowing and line-of-sight components has not yet been presented in the literature. The most important results of the paper are summarised in Section 4.

2 System Model and Basic Assumptions

Consider a simulcast network according to Fig. 1 consisting of n base stations (BS₁ to BS _{n}) which transmit signals $s_1(t), \dots, s_n(t)$ to a mobile receiver (MS) with fixed random position. For simplicity, we assume that the base stations and the mobile receiver are equipped with just a single antenna. In order to provide a microscopic spatial diversity gain, the base stations employ a distributed space-time block coding (STBC) scheme.

Throughout this paper, the complex baseband notation is used. Assuming a quasi-static frequency-flat² fading channel model, we model the transmission link from the i th base station to the mobile receiver by a single complex-valued channel coefficient $h_i \triangleq \alpha_i e^{j\varphi_i}$, which is constant over the duration of an entire data block. After each data block, the channel coefficients change randomly, while h_i and $h_{i'}$ ($i \neq i'$) are statistically independent. For the time being, we assume that the differences between the propagation delays of the signals $s_1(t), \dots, s_n(t)$ are small compared to the symbol duration.³ The discrete-time channel model is therefore given by

$$y[k] = \sum_{i=1}^n h_i x_i[k] + n[k], \quad (1)$$

²The results presented in this paper are also relevant for frequency-selective channel models. For example, they can directly be applied to space-time block coded orthogonal-frequency-division-multiplexing (OFDM) systems.

³The case of large relative propagation delays is discussed in Section 3.3.

where k denotes the discrete time index, $y[k]$ the k th received sample, $x_i[k] \in \mathbb{C}$ the k th transmitted symbol of base station BS_i , and $n[k]$ a sample of a complex additive white Gaussian noise (AWGN) process with zero mean and variance $\sigma_n^2/2$ per real dimension, i.e., $n[k] \sim \mathcal{CN}(0, \sigma_n^2)$. The transmitted symbols $x_i[k]$ represent space-time encoded information symbols $a[k]$, which are assumed to be (randomly) drawn from an M -ary symbol alphabet, e.g., an M -ary phase-shift-keying (PSK) constellation. Throughout this paper it is assumed that the noise samples, the data symbols, and the channel coefficients are statistically independent.

In a simulcast network used for broadcasting applications, many users are simultaneously served with the same message. Correspondingly, it is not useful to optimise the transmission strategy with respect to a specific user. Similarly, in a paging application a single user with unknown position is served. In this case, an optimisation of the transmission strategy is not feasible. In both scenarios, it is therefore reasonable to employ an equal power allocation strategy at the transmitter side, i.e., the individual base stations use the same average transmit power $P_{\text{Tx},i} \triangleq \mathbb{E}\{|x_i[k]|^2\}$ ($\mathbb{E}\{\cdot\}$ denotes statistical expectation). For the purpose of analysis, we assume that the overall transmit power $P \triangleq \sum_i P_{\text{Tx},i}$ is fixed, irrespective of the number of transmit antennas used. This allows for a fair comparison with a single-antenna system.

The instantaneous and the average received signal-to-noise ratio (SNR) for the i th transmission link (per channel use) is given by

$$\gamma_i \triangleq \frac{P}{n} \frac{\alpha_i^2}{\sigma_n^2}, \quad \bar{\gamma}_i \triangleq \mathbb{E}\{\gamma_i\} = \frac{P}{n} \frac{\Omega_i}{\sigma_n^2}, \quad (2)$$

respectively, where $\Omega_i \triangleq \mathbb{E}\{\alpha_i^2\}$ denotes the average power of the i th channel coefficient. For a fair comparison between a system with distributed transmitters and a system with co-located transmitters, the overall average received SNR must be fixed. Correspondingly, we apply the normalisation $\sum_i \Omega_i \stackrel{!}{=} n$ throughout this paper. (In the case of co-located transmitters, it is reasonable to assume that the parameters Ω_i are equal for all i , whereas in a distributed system they may be different from one link to another, due to different link lengths.) With this normalisation, the overall average received SNR results as

$$\bar{\gamma}_{\text{ov}} \triangleq \sum_{i=1}^n \bar{\gamma}_i = \frac{P}{\sigma_n^2}. \quad (3)$$

In the following, let $\bar{\gamma}_{\text{ov}} \triangleq E_s/N_0$, where E_s denotes the (overall) average received symbol energy per channel use and N_0 the single-sided noise power density.

2.1 Distributed Space-Time Code

Within the scope of this paper, the base stations are assumed to employ a distributed orthogonal space-time block code (OSTBC) [2],[3]. OSTBCs yield full spatial diversity with regard to the number of transmit and receive antennas available. In the flat-fading case, OSTBCs enable maximum-likelihood decoding at the receiver by means of simple linear processing. A drawback of these schemes is, however, that a temporal rate $R_t=1$ (‘full rate’) is only accomplished for certain numbers of transmit antennas. Given a two-dimensional signal constellation (e.g., an M -PSK constellation), full-rate transmission is, in fact, only accomplished by Alamouti’s OSTBC [2] for $n=2$ transmitters [13]. In the case of $n=3$ and $n=4$ transmitters, for example, the maximum possible rate is $R_t=3/4$ [3],[4].

2.2 Fading Models

In order to model the effects of microscopic fading, random fading amplitudes α_i are considered that are either characterised by a Rayleigh distribution (i.e. $h_i \sim \mathcal{CN}(0, \Omega_i)$) or by a Rician distribution. The Rician distribution is used to model the effect of a line-of-sight (LOS) signal component. In this case, the channel coefficients h_i can be written as $h_i \triangleq h_{\text{LOS},i} + \tilde{h}_i$, where $h_{\text{LOS},i} \in \mathbb{C}$ represents the non-fading LOS component⁴ and $\tilde{h}_i \sim \mathcal{CN}(0, \tilde{\Omega}_i)$ the scattered components ($\Omega_i \triangleq |h_{\text{LOS},i}|^2 + \tilde{\Omega}_i$). The Rice factor $K_i \in [0, \infty[$ is defined as the ratio between LOS signal power and average power of the scattered components, i.e., $K_i = |h_{\text{LOS},i}|^2 / \tilde{\Omega}_i$. The cases $K_i=0$ and $K_i \rightarrow \infty$ correspond to pure Rayleigh fading and a non-fading AWGN link, respectively. The probability density function (PDF) $p_{\Gamma_i}(\gamma_i)$ of the instantaneous SNR γ_i for the case of Rayleigh fading is given by

$$p_{\Gamma_i}(\gamma_i) = \frac{1}{\tilde{\gamma}_i} \exp\left(-\frac{\gamma_i}{\tilde{\gamma}_i}\right). \quad (4)$$

The corresponding PDF for the case of Rician fading can be found in [14].

⁴According to the quasi-static fading assumption, the phase of the LOS component is assumed to change randomly from one data block to the next.

To account for macroscopic fading in terms of shadowing effects, the average SNRs $\bar{\gamma}_i$ themselves are regarded as random variables characterised by a log-normal distribution. This means that the average SNR in dB, $\bar{\gamma}_{\text{dB},i} \triangleq 10 \log_{10} \bar{\gamma}_i$ dB, is assumed to be Gaussian distributed. In the sequel, let $\mu_{\text{dB},i}$ and $\sigma_{\text{dB},i}^2$ denote the mean and the variance of $\bar{\gamma}_{\text{dB},i}$ in dB, respectively, i.e., $\bar{\gamma}_{\text{dB},i} \sim \mathcal{N}(\mu_{\text{dB},i}, \sigma_{\text{dB},i}^2)$. To combine Rayleigh fading with log-normal shadowing, the PDF (4) is conditioned on $\bar{\gamma}_i$ and then averaged over the log-normal PDF of $\bar{\gamma}_i$ [14].

In Fig. 2, some example PDFs $p_{\Gamma_i}(\gamma_i)$ are shown for Rician fading as well as for composite Rayleigh fading/ log-normal shadowing ($\bar{\gamma}_i = 1$ in all cases). The PDF for $\sigma_{\text{dB},i} = 1$ dB represents very light shadowing, i.e., $p_{\Gamma_i}(\gamma_i)$ is virtually the same as for pure Rayleigh fading ($p_{\Gamma_i}(\gamma_i) \approx \exp(-\gamma_i)$). As can be seen in Fig. 2, when shadowing is more severe (e.g. $\sigma_{\text{dB},i} = 10$ dB), the probability of small instantaneous SNR values increases significantly.

*** Fig. 2 about here ***

3 Error Performance of Distributed OSTBCs Under Shadowing and Line-of-Sight Components

Consider again the system model according to (1). The employed OSTBC (in conjunction with an appropriate linear detector at the receiver side) transforms the system with n transmit antennas and one receive antenna⁵ (in the sequel denoted as $(n \times 1)$ -system) into an equivalent single-antenna system of form [15]

$$z[k] = \left(\sum_{i=1}^n |h_i|^2 \right)^{1/2} a[k] + w[k], \quad (5)$$

where $z[k]$ denotes the k th received sample at the output of the linear detector, $a[k]$ the k th information symbol before the OSTBC, and $w[k]$ a sample of a complex AWGN process with zero mean and variance $\sigma_n^2/2l$ per real dimension, i.e., $w[k] \sim \mathcal{CN}(0, \sigma_n^2/l)$.⁶ Altogether, the $(n \times 1)$ -OSTBC system (with linear detector) is equivalent to a $(1 \times n)$ -

⁵It is straightforward to generalise this concept to OSTBC systems with multiple receive antennas.

⁶The parameter l depends on the OSTBC under consideration [15]. For example, for Alamouti's OSTBC [2] as well as for the OSTBCs proposed in [3],[4] for three and four transmit antennas, $l=1$ results. For the half-rate OSTBCs proposed in [3], we have $l=2$.

system with maximum-ratio combining (MRC) at the receiver side and an average transmit power of P/nR_t (given equivalent fading statistics and a noise variance of σ_n^2 per receive antenna). Taking the temporal rate of the OSTBC into account, the overall average received SNR per information symbol $a[k]$ is given by

$$\bar{\gamma}'_{ov} = \sum_{i=1}^n \bar{\gamma}'_i \triangleq \frac{\bar{\gamma}_{ov}}{R_t}. \quad (6)$$

The average received SNR per information bit is in the sequel denoted as

$$\frac{E_b}{N_0} \triangleq \frac{\bar{\gamma}'_{ov}}{\log_2(M)} = \frac{\bar{\gamma}_{ov}}{R_t \log_2(M)}, \quad (7)$$

where E_b denotes the average received energy per information bit.

Using the analytical framework presented in [14], the average symbol error probability of the OSTBC-system with linear detector can be determined analytically by evaluating a finite-range integral. (The instantaneous SNRs γ'_i of the individual transmission links are statistically independent.) For example, in the case of an M -PSK signal constellation, the average symbol error probability, \bar{P}_s , can be written as

$$\bar{P}_s = \frac{1}{\pi} \int_0^{\frac{(M-1)\pi}{M}} f(\phi) d\phi. \quad (8)$$

(For quadrature-amplitude-modulation (QAM) and amplitude-shift-keying (ASK) constellations similar expressions can be found in [14]. For simplicity, we focus on M -PSK constellations here.) This general equation holds for arbitrary fading statistics of the individual transmission links. The function $f(\phi)$ is directly related to the PDFs of the instantaneous SNRs γ'_i :

$$f(\phi) \triangleq \prod_{i=1}^n \underbrace{\int_0^\infty p_{\Gamma'_i}(\gamma'_i) \exp\left(-\frac{g\gamma'_i}{\sin^2(\phi)}\right) d\gamma'_i}_{\triangleq f_i(\phi)}, \quad (9)$$

where $g \triangleq \sin^2(\pi/M)$. Note that $f_i(\phi) \geq 0$ for all ϕ . In many cases, closed-form expressions are known for the functions $f_i(\phi)$ [14]. For example, for Rician fading we have

$$f_i(\phi) = \frac{\xi_i(\phi)}{\xi_i(\phi) + g\bar{\gamma}'_i} \exp\left(-\frac{K_i g \bar{\gamma}'_i}{\xi_i(\phi) + g\bar{\gamma}'_i}\right), \quad (10)$$

where $\xi_i(\phi) \triangleq (1 + K_i) \sin^2(\phi)$. (In the case of binary transmission ($M=2$) and pure Rayleigh fading, there are even closed-form expressions for \bar{P}_s [16, Ch. 14].)

In the sequel, numerical performance results are presented for distributed OSTBCs. Specifically, the influence of line-of-sight components and shadowing on the symbol error performance is analysed and compared to OSTBC systems with co-located transmitters.

3.1 Influence of Line-of-Sight Components

Consider a system with n distributed transmitters and a single receiver where all transmission links are characterised by Rayleigh fading (Rice-factor $K_i = 0$ for all indices i). In the following, it will be seen that the average symbol error probability is already significantly improved, if only a single link i' contains a line-of-sight component ($K_{i'} > 0$). This becomes evident when examining the corresponding function $f_{i'}(\phi)$, cf. (9)-(10). For $K_{i'} > 0$, the PDF $p_{\Gamma_{i'}}(\gamma'_{i'})$ is less concentrated at small values of $\gamma'_{i'}$ than for $K_{i'} = 0$. This can be seen in Fig. 2 for the example $K_{i'} = 10$ (light colour), while the case $K_{i'} = 0$ is in essence represented by the PDF for Rayleigh fading with $\sigma_{\text{dB},i} = 1$ (dashed-dotted line, dark colour). To obtain the function $f_{i'}(\phi)$, the PDF $p_{\Gamma_{i'}}(\gamma'_{i'})$ is (for each value of ϕ) multiplied with the term $\exp(-g\gamma'_{i'}/\sin^2(\phi))$ and integrated over $\gamma'_{i'}$, cf. (9). Since for any value of ϕ the exponential term decreases with growing $\gamma'_{i'}$, the area under the function $p_{\Gamma_{i'}}(\gamma'_{i'}) \exp(-g\gamma'_{i'}/\sin^2(\phi))$ tends to be smaller when $K_{i'}$ is greater than zero. Correspondingly, the functions $f_{i'}(\phi)$ and $f(\phi)$ are smaller, i.e., the average symbol error probability \bar{P}_s according to (8) is reduced.

*** Fig. 3 and Fig. 4 about here ***

This fact is illustrated in Fig. 3, where the function $f(\phi)$ is displayed for the example of $n = 4$ transmitters, given different PSK constellations with cardinalities $M = 2, 4, 8$ (solid, dashed, and dashed-dotted curves, respectively). For simplicity, it has been assumed that the average power Ω_i is the same for all transmission links. (The case of unequal average powers Ω_i is considered in Section 3.3.) Two different cases are depicted: (i) Rice factors $K_i = 0$ for all indices i (pure Rayleigh fading, dark curves); (ii) Rice factors $K_{i'} = 10$ and $K_i = 0$ for all indices $i \neq i'$ (light colour). As can be seen, for all considered PSK constellations the area under the function $f(\phi)$ is reduced significantly, when a single line-of-sight component with $K_{i'} = 10$ is present (since the graphs for $K_{i'} = 10$ are always significantly below the corresponding graphs for pure Rayleigh fading).

For the case of binary transmission, corresponding bit error rate (BER) results are presented in Fig. 4 (also for the case that more than one link is characterised by a Rice-factor of $K_i=10$). The exact analytical results for the average bit error probability according to (8) and (9) are plotted versus E_b/N_0 in dB. For the OSTBC a temporal rate of $R_t=3/4$ was assumed, i.e., $10 \log_{10}(E_b/N_0) \text{ dB} = 10 \log_{10}(E_s/N_0) \text{ dB} + 1.25 \text{ dB}$.

In a system with co-located transmitters, one can assume that either all links simultaneously contain a line-of-sight component (dashed line, light colour) or none of them (dashed line, dark colour). The line-of-sight probability is therefore (more or less) the same as in a (1×1)-system, i.e., the use of multiple antennas does not yield any advantage in this respect. In a system with distributed transmitters, however, there is a comparably high probability that at least one link contains a line-of-sight component. As can be seen, already a single link with a Rice factor of $K_i=10$ (dashed-dotted line, dark colour) yields a gain of about 1.8 dB compared to the case of pure Rayleigh fading (at a BER of 10^{-4}).

3.2 Influence of Shadowing

In the sequel, we consider Rayleigh fading⁷ in conjunction with log-normal shadowing, i.e., the average SNRs $\bar{\gamma}'_{\text{dB},i}$ in dB are assumed to be Gaussian distributed with mean $\mu'_{\text{dB},i} = 10 \log_{10} \bar{\gamma}'_i \text{ dB}$ and variance $\sigma_{\text{dB},i}^2$. Unfortunately, a closed-form expression for the corresponding function $f_i(\phi)$ is not known in this case [17], i.e., an analytical evaluation of the average symbol error probability \bar{P}_s is difficult. Correspondingly, we resort to numerical performance results obtained by Monte-Carlo simulations.

With regard to shadowing, the use of multiple co-located transmit antennas is again not advantageous. Large-scale objects between transmitter and receiver will most likely obstruct either all links simultaneously or none of them. Therefore, the probability of shadowing is not significantly reduced compared to a (1×1)-system. In other words, the average SNRs $\bar{\gamma}'_{\text{dB},i}$ will be strongly correlated. In a system with distributed transmitters, however, the average SNRs $\bar{\gamma}'_{\text{dB},i}$ can be assumed statistically independent [18], which yields huge (macroscopic) diversity gains.

This is illustrated in Fig. 5 for the example of $n=4$ transmitters, binary transmission,

⁷The results presented in the following apply, in principle, also for Nakagami- m fading [14] with fading parameter $m \neq 1$ (the case $m=1$ represents Rayleigh fading).

and identical average channel powers Ω_i and variances $\sigma_{\text{dB},i}^{\prime 2}$ for all links. In the case of co-located transmitters, it was assumed for simplicity that the average SNRs $\bar{\gamma}'_{\text{dB},i}$ are fully correlated, i.e.

$$\text{E}\{(\bar{\gamma}'_{\text{dB},i} - \mu'_{\text{dB},i})(\bar{\gamma}'_{\text{dB},i'} - \mu'_{\text{dB},i'})\} / \sigma_{\text{dB},i}^{\prime 2} = 1 \quad (11)$$

for all indices i and i' . In the case of very light shadowing ($\sigma'_{\text{dB},i} = 1$ dB), the BER performance with distributed transmitters is virtually the same as with co-located transmitters (as expected). In both cases, significant (microscopic) diversity gains are obtained compared to the (1×1)-system. (Since the shadowing effect is negligible, the composite fading is virtually independent for the individual links, both for co-located and for distributed transmitters.) Considering a more practical scenario ($\sigma'_{\text{dB},i} = 10$ dB), one first observes that the performance of the (1×1)-system degrades significantly. The use of $n = 4$ co-located transmit antennas yields only moderate performance improvements, i.e., a large portion of the microscopic diversity gain obtained for $\sigma'_{\text{dB},i} = 1$ dB is lost. As opposed to this, in the case of distributed transmitters one again obtains huge diversity gains compared to the (1×1)-system. These gains are not only due to macroscopic diversity, but also to microscopic diversity accomplished by the distributed OSTBC. This becomes evident, when comparing the BER performance⁸ to that of conventional simulcasting⁸ (dotted curve). As can be seen, conventional simulcasting performs about 1.5 dB worse than the distributed OSTBC (at a BER of 10^{-3}).

*** Fig. 5 about here ***

Another interesting observation is that for low SNR values the BER performance of a distributed OSTBC system with significant shadowing ($\sigma'_{\text{dB},i} = 10$ dB) is even better than for very light shadowing ($\sigma'_{\text{dB},i} = 1$ dB), which is a rather unexpected result. There is a cross-over point of the respective BER curves at 3.5 dB. (In the case $n = 1$, there is also a cross-over point at approximately -2.5 dB.) An intuitive explanation for this is as follows: In the low SNR regime channel conditions are already bad, and a further reduction of the SNR due to shadowing does not have much impact on the BER performance. However, a large variance $\sigma_{\text{dB},i}^{\prime 2}$ of the average SNR $\bar{\gamma}'_{\text{dB},i}$ leads to

⁸To be specific, an improved version of simulcasting is already considered here, where the phases of the individual transmitted signals are adjusted such that constructive superposition is obtained at the receiver.

some very good channel realisations, which is obviously beneficial for the average BER performance. This cross-over behaviour can also be observed when considering the corresponding functions $f_i(\phi)$, cf. (9): In the case of moderate to high SNR values (e.g. $\bar{\gamma}'_i = 1$), the PDFs $p_{\Gamma'_i}(\gamma'_i)$ are less concentrated at small values of γ'_i , when the variance $\sigma_{\text{dB}_i}^{2'}$ is small (cf. Fig. 2). Correspondingly, the function $f(\phi)$ – and thus the average bit error probability \bar{P}_b – is smaller than for large variances $\sigma_{\text{dB}_i}^{2'}$. In the case of low SNR values, however, the PDF $p_{\Gamma'_i}(\gamma'_i)$ is already concentrated at very small values γ'_i . Given a large variance $\sigma_{\text{dB}_i}^{2'}$, the PDF $p_{\Gamma'_i}(\gamma'_i)$ exhibits a tail that tends to higher values of γ'_i (not depicted in Fig. 2). Due to this, the function $f(\phi)$ and thus the average bit error probability \bar{P}_b becomes smaller with growing variance $\sigma_{\text{dB}_i}^{2'}$.

3.3 Impact of Unequal Link Lengths

For the numerical results presented above, we have assumed that the average channel power Ω_i is the same for all transmission links. In a system with distributed transmitters, however, the individual link lengths d_i will in general be different. Since the received power scales with $1/d_i^p$, where $2 \leq p \leq 4$ in practical scenarios [19, Ch. 1.2], already small differences in the link lengths cause significant differences in the received powers. This effect is in the sequel modelled by unequal average channel powers Ω_i .

As an example, we revisit the BER results presented in Fig. 5 and consider the case of unequal average channel powers $\Omega_i = \{3.08, 0.62, 0.15, 0.15\}$. The corresponding BERs are displayed in Fig. 6. As can be seen, the BER performance of the distributed system is significantly degraded due to the unequal average channel powers (cf. Fig. 5). In the case of light shadowing ($\sigma'_{\text{dB},i} = 1$ dB), where the achieved diversity gains are mainly due to microscopic spatial diversity, the OSTBC system with co-located transmit antennas thus clearly outperforms the distributed OSTBC system. However, in the case of significant shadowing ($\sigma'_{\text{dB},i} = 10$ dB) the situation is reversed: Due to huge macroscopic diversity gains, the distributed OSTBC system still yields a much better BER performance than the system with co-located transmit antennas. Moreover, the advantage of the distributed OSTBC over conventional simulcasting is maintained.

*** Fig. 6 about here ***

If the individual transmitters are spaced very far apart, large differences can occur

between the individual link lengths d_i . In this case, the assumption that the differences between the corresponding propagation delays are small compared to the symbol duration might not be valid anymore. Therefore, if no timing-advance techniques are applied at the transmitter side, intersymbol interference (ISI) effects can occur at the receiver. Since OSTBCs were designed for channels without ISI, this can cause significant performance degradations which compromise the achieved diversity gains. One option to solve this problem is to employ an appropriate equaliser algorithm at the receiver, so as to mitigate the impact of ISI. For example, a trellis-based equalisation/ detection algorithm for Alamouti's OSTBC was presented in [20]. Alternatively, the OSTBC may be replaced by space-time coding techniques that are suitable for ISI channels, such as the time-reversal STBC scheme in [21]. In both cases, the main results of Section 3.1 and 3.2 will still be valid.

4 Conclusions

In this paper, we have analysed the error performance of distributed space-time codes in a mobile broadcasting system with multiple base stations. Due to the distributed nature of the system, mobile users within the intersection of the individual coverage areas are provided with a comparably high line-of-sight probability. Our analysis has shown that already a single link with line of sight significantly improves the overall error performance of the system. With regard to shadowing, it has been shown that huge macroscopic and microscopic diversity gains can be obtained in a space-time coded system with distributed transmitters. In a system with co-located transmitters, however, the performance improvements compared to a single-antenna system are rather small, when shadowing is taken into account. To conclude, mobile broadcasting systems with distributed transmitters are typically superior to conventional multiple-antenna systems, due to macroscopic diversity. Moreover, distributed space-time codes are superior to conventional simulcasting, even in the case of severe shadowing and unequal signal-to-noise ratios on the individual transmission links.

References

- [1] Tarokh, V., Seshadri, N., and Calderbank, A. R.: ‘Space-time codes for high data rate wireless communication: Performance criterion and code construction’, *IEEE Trans. Inform. Theory*, 1998, **44**, (2), pp. 744-765
- [2] Alamouti, S. M.: ‘A simple transmit diversity technique for wireless communications’, *IEEE J. Select. Areas Commun.*, 1998, **16**, (8), pp. 1451-1458
- [3] Tarokh, V., Jafarkhani, H., and Calderbank, A. R.: ‘Space-time block coding for wireless communications: Performance results’, *IEEE J. Select. Areas Commun.*, 1999, **17**, (3), pp. 451-460
- [4] Tirkkonen, O., and Hottinen, A.: ‘Complex space-time block codes for four Tx antennas’. Proc. IEEE Global Telecommun. Conf. (Globecom), San Francisco, CA, USA, Nov./Dec. 2000, pp. 1005-1009
- [5] Brennan, D. G.: ‘Linear diversity combining techniques’, *Proc. IRE*, 1959, **47**, pp. 1075-1102
- [6] Wittneben, A.: ‘Basestation modulation diversity for digital Simulcast’. Proc. IEEE Veh. Technol. Conf. (VTC), St. Louis, MO, USA, May 1991, pp. 848-853
- [7] Anghel, P. A., Leus, G., and Kaveh, M.: ‘Distributed space-time coding in cooperative networks’. Proc. V IEEE Nordic Signal Processing Symposium (NORSIG), Oct. 2002, paper no. SunAmOR2-2
- [8] Kastrisios, A., Dohler, M., and Aghvami, H.: ‘Influence of channel characteristics on the performance of VAA with deployed STBCs’. Proc. IEEE Veh. Technol. Conf. (VTC-Spring), Jeju, Korea, April 2003, pp. 1138-1142
- [9] Laneman, J. N., and Wornell, G. W.: ‘Distributed space-time-coded protocols for exploiting cooperative diversity in wireless networks’, *IEEE Trans. Inform. Theory*, 2003, **49**, (10), pp. 2415-2425
- [10] Sendonaris, A. , Erkip, E., and Aazhang, B.: ‘User cooperation diversity – Part 1: System description; Part 2: Implementation aspects and performance analysis’, *IEEE Trans. Commun.*, 2003, **51**, (11), pp. 1927-1948
- [11] Pabst, R., Walke, B. H., Schultz, D. C., Herhold, P., Yanikomeroglu, H., et. al.: ‘Relay-based deployment concepts for wireless and mobile broadband radio’, *IEEE Commun. Mag.*, 2004, **42**, (9), pp. 80-89
- [12] Mietzner, J., Thobaben, R., and Hoeher, P. A.: ‘Analysis of the expected error performance of cooperative wireless networks employing distributed space-time codes’. Proc. IEEE Global Telecommun. Conf. (Globecom), Dallas, TX, USA, Nov./Dec. 2004, pp. 2854-2858
- [13] Liang, X.-B., and Xia, X.-G.: ‘On the nonexistence of rate-one generalized complex orthogonal designs’, *IEEE Trans. Inform. Theory*, 2003, **49**, (11), pp. 2984-2989
- [14] Alouini, M.-S., and Goldsmith, A. J.: ‘A unified approach for calculating error rates of linearly modulated signals over generalized fading channels’, *IEEE Trans. Commun.*, 1999, **47**, (9), pp. 1324-1334
- [15] Shin, H., and Lee, J. H.: ‘Exact symbol error probability of orthogonal space-time block codes’. Proc. IEEE Global Telecommun. Conf. (Globecom), Taipei, Taiwan, R.O.C., Nov. 2002, pp. 1197-1201
- [16] Proakis, J. G.: ‘Digital Communications’ (4th ed., New York: McGraw-Hill, 2001)
- [17] Alouini, M.-S., and Simon, M. K.: ‘Dual diversity over correlated log-normal fading channels’, *IEEE Trans. Commun.*, 2002, **50**, (12), pp. 1946-1959
- [18] Emamian, V., Kaveh, M., and Alouini, M.-S.: ‘Outage probability with transmit and receive diversity in a shadowing environment’. Proc. IEEE Wireless Commun. and Networking Conf. (WCNC), Orlando, FL, USA, Mar. 2002, pp. 54-57
- [19] Steele, R. (Ed.): ‘Mobile Radio Communications’ (New York: IEEE Press, 1994)
- [20] Mietzner, J., Hoeher, P. A., and Sandell, M.: ‘Compatible improvement of the GSM/EDGE system by means of space-time coding techniques’, *IEEE Trans. Wireless Commun.*, 2003, **2**, (4), pp. 690-702
- [21] Lindskog, E., and Paulraj, A.: ‘A transmit diversity scheme for channels with intersymbol interference’. Proc. IEEE Int. Conf. Commun. (ICC), New Orleans, LA, USA, June 2000, pp. 307-311

Figure Captions

Fig. 1. Simulcast network consisting of multiple base stations.

Fig. 2. Some example PDFs for the instantaneous SNR γ_i . Light colour: Rician fading with Rice-factor $K_i = 10$ ($\bar{\gamma}_i = 1$). The remaining PDFs are for composite Rayleigh fading / log-normal shadowing ($\mu_{\text{dB},i} = 0$ dB, i.e. $\bar{\gamma}_i = 1$). Dashed-dotted line: $\sigma_{\text{dB},i} = 1$ dB (very light shadowing), dashed line: $\sigma_{\text{dB},i} = \sqrt{10}$ dB, solid line: $\sigma_{\text{dB},i} = 10$ dB.

Fig. 3. Function $f(\phi)$ for the example $n = 4$ with (i) Rice-factors $K_i = 0$ for all i and (ii) Rice-factors $K_{i'} = 10$ and $K_i = 0$ for $i \neq i'$ ($\bar{\gamma}'_{\text{ov}} = 10$ and $\bar{\gamma}'_i = \bar{\gamma}'_{\text{ov}}/4$ for all i). Solid lines: 2-PSK modulation; dashed lines: 4-PSK modulation; dashed-dotted lines: 8-PSK modulation. The respective areas under the curves represent the average symbol error probability \bar{P}_s .

Fig. 4. Analytical results for the BER performance of a distributed OSTBC system with $n = 4$ transmitters and a single receiver (binary transmission, $\bar{\gamma}'_i = \bar{\gamma}'_{\text{ov}}/4$ for all i): One or more links have a line-of-sight component with a Rice factor of $K_i = 10$, while the remaining links are characterised by Rayleigh fading ($K_i = 0$).

Fig. 5. Comparison of the BER performance of a co-located and a distributed OSTBC system with $n = 4$ transmitters and a single receiver (binary transmission, equal average SNRs $\bar{\gamma}'_i$): Composite Rayleigh fading / log-normal shadowing with $\sigma_{\text{dB},i} = 1$ dB (very light shadowing) and $\sigma_{\text{dB},i} = 10$ dB, respectively. The dotted curve is for conventional simulcasting with co-phased received signals ($\sigma_{\text{dB},i} = 10$ dB).

Fig. 6. Comparison of the BER performance of a co-located and a distributed OSTBC system with $n = 4$ transmitters and a single receiver (binary transmission, unequal average SNRs $\bar{\gamma}'_i$): Composite Rayleigh fading / log-normal shadowing ($\sigma_{\text{dB},i} = 1$ dB and $\sigma_{\text{dB},i} = 10$ dB), average channel powers $\Omega_i = \{3.08, 0.62, 0.15, 0.15\}$ considered. The dotted curve is for conventional simulcasting with co-phased received signals ($\sigma_{\text{dB},i} = 10$ dB).

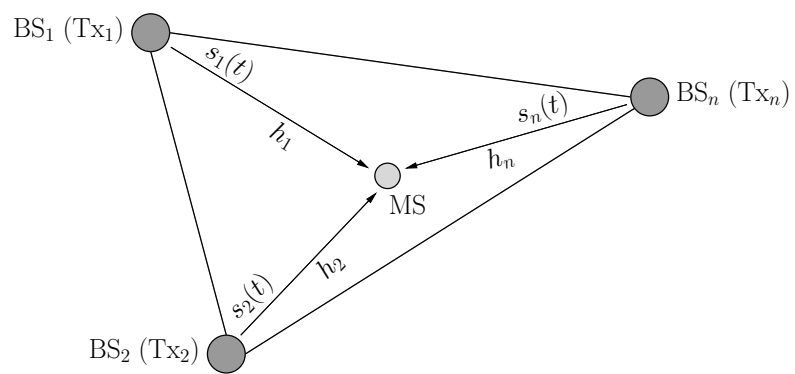


Fig. 1

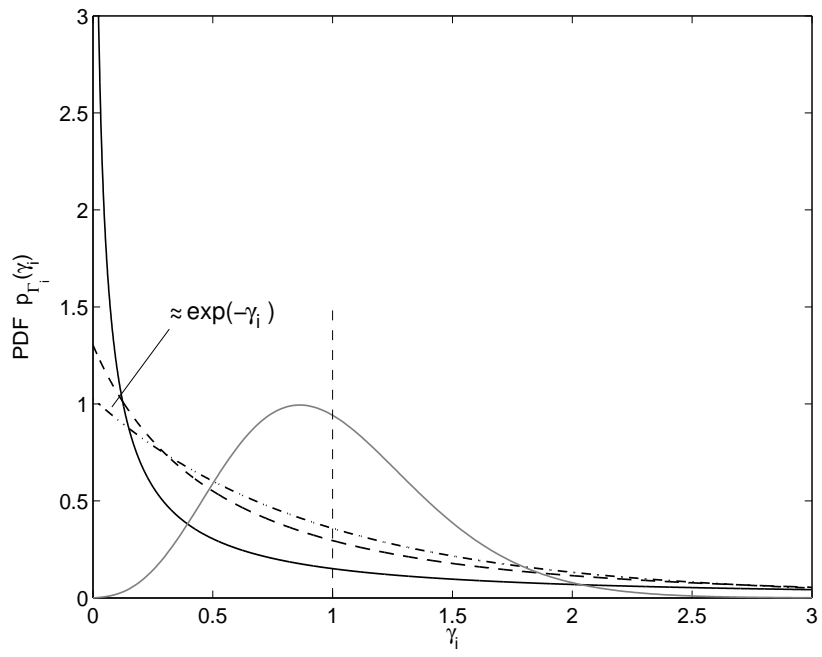


Fig. 2

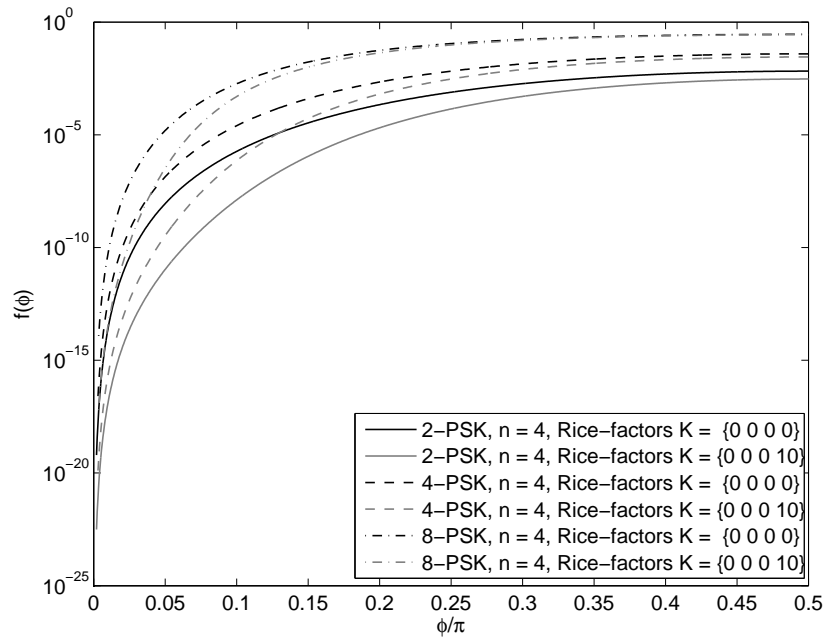


Fig. 3

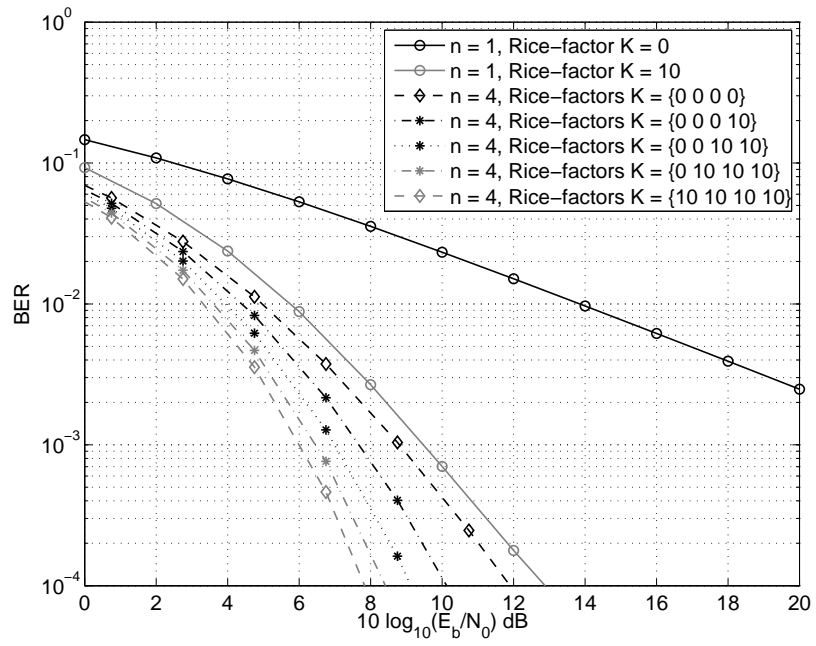


Fig. 4

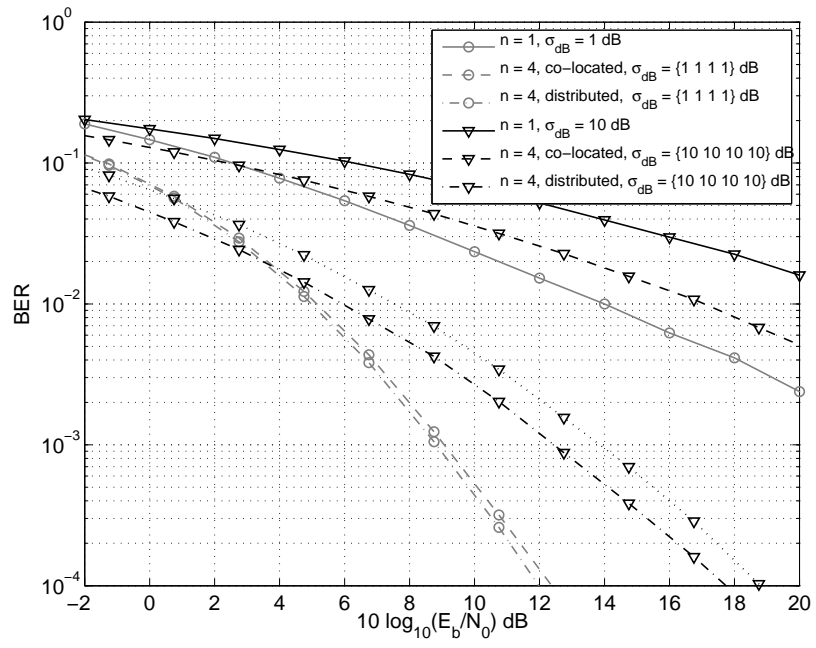


Fig. 5

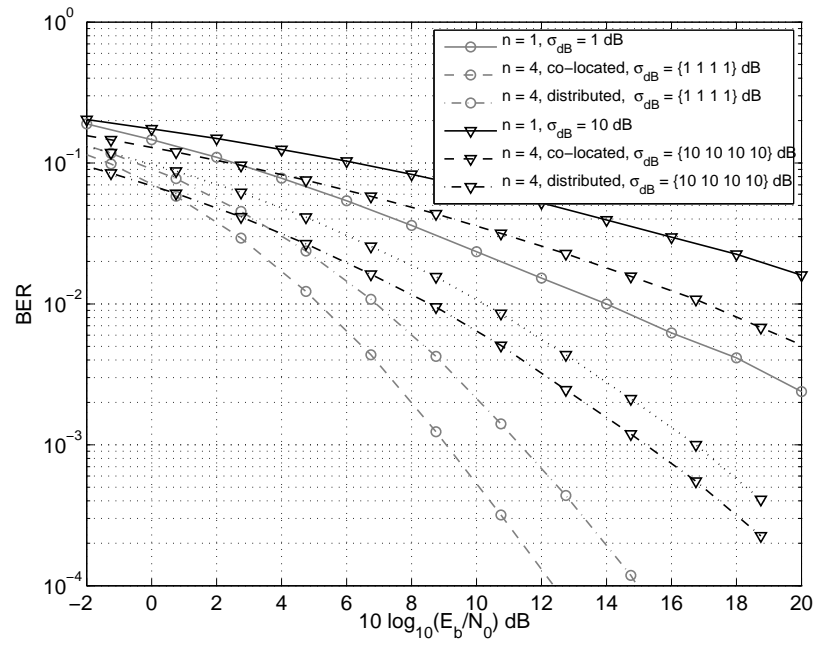


Fig. 6